Paclitaxel-Dependent Cell Lines Reveal a Novel Drug Activity

Anutosh Ganguly, Hailing Yang, and Fernando Cabral

Abstract

We previously described the isolation of Tax 18 and Tax 11-6, two paclitaxel-dependent cell lines that assemble low amounts of microtubule polymer and require the drug for cell division. In the present studies, fluorescence time-lapse microscopy was used to measure microtubule dynamic instability behavior in these cells. The mutations were found to cause small decreases in microtubule growth and shortening, but the changes seemed unable to explain the defects in microtubule polymer levels or cell division. Moreover, paclitaxel further suppressed microtubule dynamics at low drug concentrations that were insufficient to rescue the mutant phenotype. Wild-type (WT) cells treated with similar low drug concentrations also had highly suppressed microtubules, yet experienced no problems with cell division. Thus, the effects of paclitaxel on microtubule dynamics seemed to be unrelated to cell division in both WT and mutant cell lines. The higher drug concentrations needed to rescue the mutant phenotype instead inhibited the formation of unstable microtubule fragments that appeared at high frequency in the drug-dependent, but not WT, cell lines. Live cell imaging revealed that the fragments were generated by microtubule detachment from centrosomes, a process that was reversed by paclitaxel. We conclude that paclitaxel rescues mutant cell division by inhibiting the detachment of microtubule minus ends from centrosomes rather than by altering plus-end microtubule dynamics. *Mol Cancer Ther; 9(11); 2914–23. ©2010 AACR.*

Introduction

Microtubules are essential cytoskeletal components that are involved in a diverse array of cellular activities, including cell motility, cytoplasmic vesicle transport, and construction of the mitotic spindle apparatus needed for chromosome segregation and cell division. Structurally, they appear as long hollow tubes assembled from protofilaments that contain repeating units of αβ tubulin heterodimers. This repeating pattern imparts polarity in which microtubule plus ends grow out toward the cell periphery, whereas their minus ends remain embedded in organelles called centrosomes that act as nucleating centers and organizers for the microtubule cytoskeleton (1). The plus ends are highly dynamic; they display stochastic episodes of growth and shortening, interspersed with pauses in which there is no change in microtubule length. This behavior, referred to as dynamic instability, is thought to be controlled by the phosphorylation state of guanine nucleotides bound to the β-tubulin subunits at the microtubule plus ends (2).

Drugs that target tubulin are important in the treatment of cancer. They kill tumor cells by altering mitotic spindle function, thereby disrupting chromosome segregation, inhibiting mitotic progression, and preventing cell division. The drugs fall into two major groups: Some, such as colcemid and vinblastine, inhibit microtubule assembly, whereas others, such as paclitaxel and epothilones A and B, promote microtubule assembly. In spite of these differing effects on microtubule polymerization, all of the drugs suppress microtubule dynamic behavior and it is thought that this action is responsible for the ability of the drugs to inhibit mitosis (3).

We and others have described the isolation of cell lines resistant to paclitaxel that are also dependent on the presence of the drug for cell division (4, 5). These cells have mutations in α- or β-tubulin that reduce the steady-state level of microtubule polymer, interfere with mitotic spindle function, and prevent cell division (6, 7). The presence of appropriate concentrations of microtubule-stabilizing drugs such as paclitaxel, but not microtubule-destabilizing drugs such as colcemid, reverses the mutant phenotype and allows normal cell proliferation. To determine how microtubule assembly and function are altered in the mutant cell lines, we measured microtubule dynamics in the presence and absence of paclitaxel and report that changes in microtubule dynamics do not explain the mutant phenotype or its reversal by paclitaxel. Instead, we show that mutant cells produce fragments generated by microtubule detachment from centrosomes, and that paclitaxel rescues the mutants by inhibiting this process.

Authors' Affiliation: Department of Integrative Biology and Pharmacology, University of Texas Medical School, Houston, Texas

Note: Supplementary material for this article is available at Molecular Cancer Therapeutics Online (http://mct.aacrjournals.org/).

A. Ganguly and H. Yang contributed equally to this work.

Corresponding Author: Fernando Cabral, Department of Integrative Biology and Pharmacology, The University of Texas Medical School, 6431 Fannin St., Houston, TX 77030. Phone: 713-500-7485; Fax: 713-500-7456. E-mail: fernando.r.cabral@uth.tmc.edu

doi: 10.1158/1535-7163.MCT-10-0552

Materials and Methods

Cell lines

Parental Chinese hamster ovary (CHO) cells were grown at 37°C and 5% CO_2 in α-MEM with 5% fetal bovine serum (Gemini Bio-Products), 50 units/mL penicillin, and 50 μg/mL streptomycin as previously described (8). Paclitaxel-dependent CHO cell lines were maintained in the same culture medium supplemented with 200 nmol/L paclitaxel (Supplementary Fig. S1). All reagents were from Sigma-Aldrich unless otherwise stated.

Immunofluorescence

Cells were seeded onto sterile glass coverslips in the presence or absence of paclitaxel and grown for 2 days. They were then rinsed in PBS and fixed in methanol at −20°C for 20 minutes. In some cases, cells were preextracted before fixation by incubating coverslips for 1 minute at 4°C in microtubule-stabilizing buffer [20 mmol/L Tris-HCl (pH 6.8), 1 mmol/L $MgCl_2$, 2 mmol/L EGTA, 0.5% NP40] containing 4 μmol/L paclitaxel. Following fixation, cells were washed with PBS, incubated with a 1:100 dilution of mouse monoclonal antibody DM1A for 1 hour at 37°C, washed, and stained for 1 hour with a 1:100 dilution of Alexa Fluor 488–conjugated goat anti-mouse IgG (Invitrogen) that included 1 μg/mL 4′,6-diamidino-2-phenylindole (DAPI). Cells were viewed using an Optiphot microscope (Nikon, Inc.) equipped with a MagnaFire digital camera (Optronics).

Electrophoresis and Western blots

Cellular proteins were solubilized in SDS sample buffer (9), separated on 7.5% polyacrylamide minigels, and transferred to nitrocellulose membranes. Membranes were incubated with a 1:2,000 dilution of DM1A followed by a 1:2,000 dilution of Alexa Fluor 647–conjugated goat anti-mouse IgG (Invitrogen). Bands were detected by fluorescence emission using a Storm imager (Molecular Dynamics, Inc.).

Measurement of polymerized and free tubulin

Microtubule assembly was measured by modifying a previously described procedure (10). Cells were cultured in 24-well dishes for 2 days to ~70% confluence with or without paclitaxel and lysed in 200 μL of microtubule-stabilizing buffer containing 0.14 mol/L NaCl and 4 μmol/L paclitaxel to keep polymerized microtubules intact. The lysates were centrifuged at 12,000 × *g* for 10 minutes at 4°C. An equal amount of bacterial cell lysate containing glutathione *S*-transferase–tagged α-tubulin was added to supernatant and pellet fractions to monitor for possible losses of material during subsequent steps. Proteins were precipitated with 5 volumes of acetone at 4°C and then dissolved in SDS sample buffer. Equivalent volumes of each fraction were analyzed on Western blots. The percent of total tubulin polymerized into microtubules was calculated by normalizing tubulin in the supernatant and pellet fractions to the amount of glutathione *S*-transferase–α-tubulin, dividing the normalized value from the pellet by the sum of the values from supernatant and pellet, and multiplying the quotient by 100.

Transfection and live cell microscopy

For live cell microscopy, paclitaxel-dependent cells were seeded onto sterile 25-mm circular coverslips and transfected with *EGFP-MAP4* (provided by J. Olmsted, University of Rochester, Rochester, NY) using Lipofectamine (Invitrogen). After transfection, the cells were maintained in the presence or absence of paclitaxel for 2 days and then transferred to medium containing 25 mmol/L HEPES (pH 7.4) with the appropriate concentration of paclitaxel. Images were captured 5 seconds apart at 37°C using a DeltaVision Core imaging system (Applied Precision, Inc.) equipped with a charge-coupled device camera and imaging software supplied by the vendor.

Calculating microtubule dynamics

The contour distance between the plus end of a microtubule and an arbitrary reference point on the same microtubule was measured using ImageJ software and graphed as a function of time to generate life history plots. The rates of growth and shortening were calculated from the slopes of the plots using linear regression. If the change in length of a microtubule between two successive time points was >0.5 μm, it was considered real growth or shortening; otherwise, it was treated as noise. Catastrophe was defined as the transition from either growth or pause to shortening, and the catastrophe frequency was calculated as the number of transitions divided by the time spent in growth and pause. Rescue was defined as the transition from shortening to either growth or pause, and the rescue frequency was calculated as the number of such events divided by the time spent shortening. Dynamicity, an overall measure for how dynamic the microtubules behave, was calculated by dividing the total change in length (including both growth and shortening) of a microtubule by the total time the microtubule was under observation (11). Each parameter was calculated from microtubules persisting for >2 minutes and is expressed as the mean ± SE. The Student's *t* test was used to compare parameters between different cell lines and treatments. Differences were considered significant when the *P* value was <0.05.

Microtubule nucleation

Microtubule nucleation was compared in wild-type (WT) and mutant cells transfected with *EB1-GFP* (plasmid 17234; Addgene, Inc.) by counting the number of EB1 comets in a 30-μm^2 circular area around the centrosome. Measurements were averaged from 25 successive frames taken 5 seconds apart for each of

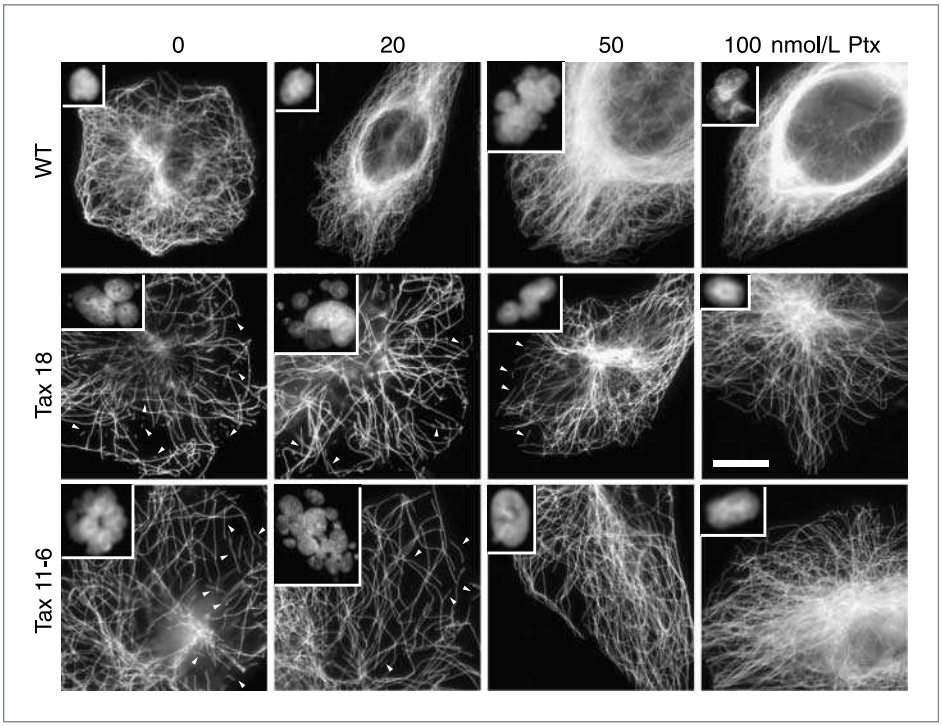

Figure 1. Effect of paclitaxel on microtubule organization and nuclear morphology. WT and paclitaxel-dependent mutants Tax 18 and Tax 11-6 were treated for 2 d with 0 to 100 nmol/L paclitaxel (Ptx) and viewed by immunofluorescence using an antibody to α-tubulin. Arrowheads point to some of the abundant microtubule fragments in the mutant cell lines cultured in low concentrations of paclitaxel. Scale bar, 10 μm. Insets, nuclear morphology. DNA was stained with DAPI and the image sizes were reduced 50% relative to their corresponding cells.

three cells from separate experiments, and the mean ± SD was calculated.

Results

Paclitaxel-dependent cell lines have reduced microtubule content

Two paclitaxel-dependent cell lines were used in this study: Tax 18 has a single L215F substitution in β1-tubulin (12), and Tax 11-6 has an E77K substitution in α-tubulin.[1] Both cell lines were isolated using single-step selections in the presence of a single cytotoxic dose of paclitaxel. The mutant phenotypes were recreated in WT CHO cells by transfection with tubulin cDNAs containing the identified mutations (12),[1] indicating that the tubulin mutations were sufficient to produce the defects observed in the mutant cell lines. Tubulin immunofluorescence of WT CHO cells and the two paclitaxel-dependent cell lines cultured for 2 days in varying concentrations of paclitaxel are shown in Fig. 1. WT cells exhibited increasing microtubule density and bundling as the concentration of paclitaxel increased. Tax 18 and Tax 11-6, on the other hand, had sparse microtubule networks that became normal as the concentration of drug increased.

Nuclear morphology is also shown in Fig. 1. Unlike HeLa and other cell lines that trigger apoptosis following a prolonged mitotic block, CHO cells with spindle defects experience a delay in mitosis, but then reenter G_1 phase without dividing and thus become large, multinucleated cells (13, 14). Multinucleation therefore serves as a convenient readout for cells that experienced problems in mitosis. WT cells exhibited multinucleation at 50 nmol/L paclitaxel and higher, thereby establishing the minimum drug concentration needed to produce defects in cell division. In contrast, the paclitaxel-dependent mutants were multinucleated in the absence of drug and required 50 or 100 nmol/L paclitaxel (Tax 11-6 and Tax 18, respectively) to restore normal nuclear morphology and cell division.

To obtain a quantitative measure of microtubule assembly, we lysed the cells in a microtubule-stabilizing buffer, centrifuged the lysate, and quantified tubulin in the pellet (microtubule) and supernatant (heterodimer) fractions. In agreement with previous experiments (10, 15), WT CHO cells assembled ~42% of their cellular tubulin into microtubules, but Tax 18 had only 15% and Tax 11-6 had 21% polymerized tubulin. The addition of 200 nmol/L paclitaxel, the drug concentration used to maintain the mutant cell cultures, raised microtubule polymer levels in the mutants back to near normal (Supplementary Table S1). It should be noted that of the two mutants, Tax 18 seemed to have the more extreme phenotype both by subjective observation and by the quantitative measurements showing that it assembles less tubulin into polymer in the absence of paclitaxel.

Microtubule dynamics are reduced in paclitaxel-dependent cell lines

To determine whether changes in dynamic behavior could account for the lower polymer levels and inability

[1] Unpublished studies.

of mutant cells to divide, we used live cell imaging to measure time-dependent changes in microtubule length. WT and mutant cells were transfected with *EGFP-MAP4* (16), and fluorescent microtubules were imaged at 5-second intervals to generate life history plots (Fig. 2). Without drug, all three cell lines exhibited significant microtubule growth and shortening phases interspersed with pauses in which length remained relatively constant (Fig. 2A–C). The only significant difference seemed to be a somewhat dampened microtubule activity in the two paclitaxel-dependent cell lines. In agreement with previous studies (17), treatment of WT cells with 50 nmol/L

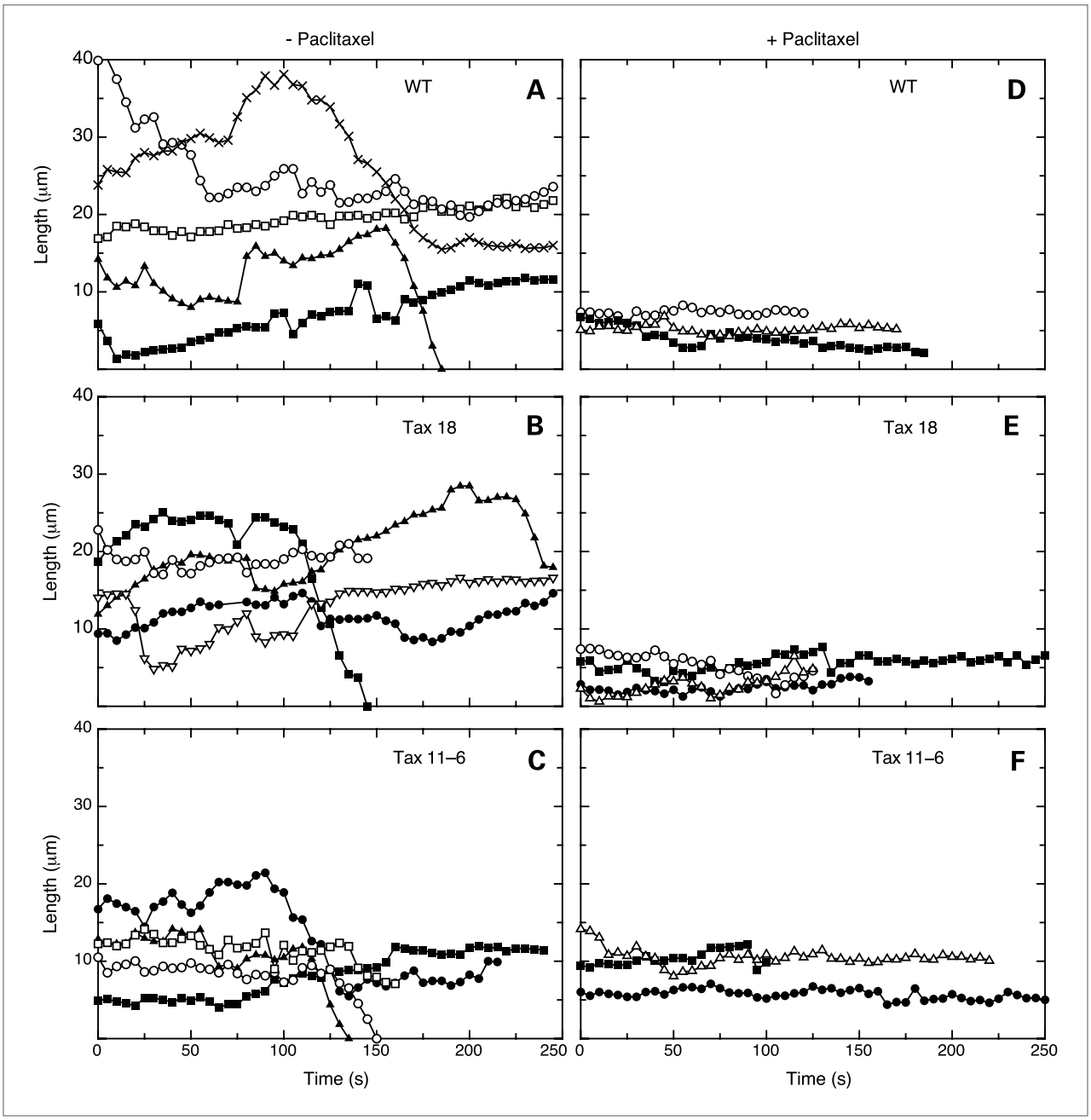

Figure 2. Microtubule life history plots. WT and mutant CHO cell lines were transfected with *EGFP-MAP4*, and fluorescent microtubules were imaged at 5-s intervals in the absence (A–C) or presence (D–F) of paclitaxel. A concentration of paclitaxel that is minimally toxic (50 nmol/L) was used to treat the WT cells, whereas mutant cells were treated with the minimum drug concentrations (50 nmol/L for Tax 11-6 and 100 nmol/L for Tax 18) needed to rescue cell division. The graphs show changes in the position of randomly chosen microtubule plus ends during the period of observation. Each line represents a single microtubule. Note that the *Y* axis represents the distance of the plus end from an arbitrary reference point and does not represent the actual total length of the microtubule. In some cases, plots were arbitrarily distributed along the *Y* axis to avoid extensive overlap.

paclitaxel, the minimum concentration needed to inhibit cell division (see Fig. 1), strongly suppressed microtubule dynamics (Fig. 2D). Contrary to expectations, however, treatment of the mutant cell lines with 50 to 100 nmol/L paclitaxel, concentrations, which restored rather than inhibited cell division, also suppressed microtubule dynamics (Fig. 2E and F). Thus, paclitaxel did not restore normal proliferation to the mutant cell lines by restoring normal microtubule dynamics.

To assess whether some aspect of microtubule behavior not immediately obvious from the life history plots could explain the mutant phenotype, we measured dynamic parameters including growth rate and duration, shortening rate and duration, time spent in a pause state, frequency of catastrophe (transition from growth or pause to shortening) or rescue (transition from shortening to growth or pause), and dynamicity (amount of growth and shortening per unit time) at a series of paclitaxel concentrations. The results are summarized in Supplementary Tables S2 to S4. We first noted that our calculated parameters for WT CHO cells in the absence of drug treatment were very similar to another study that used microinjection of rhodamine-labeled tubulin (18). This gave us confidence that both methods provide an accurate picture of microtubule behavior. Examination of the various parameters for dynamic instability, however, did not reveal changes that could easily account for the decreased amount of microtubule polymer in the mutant cells cultured without drug. Although mutant microtubule growth rates and durations were decreased relative to WT cells, so were shortening rates and durations leading to an overall lower dynamicity. Only a 40% to 50% increase in the catastrophe frequency stood out as a possible explanation for lower amounts of polymer in the mutant cells, but in Tax 11-6, the increase in catastrophe was partially offset by a 26% increase in the rescue frequency.

Changes in dynamic behavior also did not seem to correlate with the effects of paclitaxel on cell division. Maximum suppression of microtubule dynamics in WT cells occurred at paclitaxel concentrations well below the 50 nmol/L needed to cause defects in cell division; maximum suppression of microtubule dynamics in Tax 18 and Tax 11-6 occurred at concentrations well below the 50 to 100 nmol/L needed to restore them to normal cell division. Finally, we noted that similar low concentrations of paclitaxel suppressed microtubule dynamics in all three cell lines despite the fact that Tax 18 and Tax 11-6 are resistant to paclitaxel and require the drug for cell division. We concluded from these studies that changes in dynamic instability are an unlikely cause of the mutant phenotype or its reversal by paclitaxel.

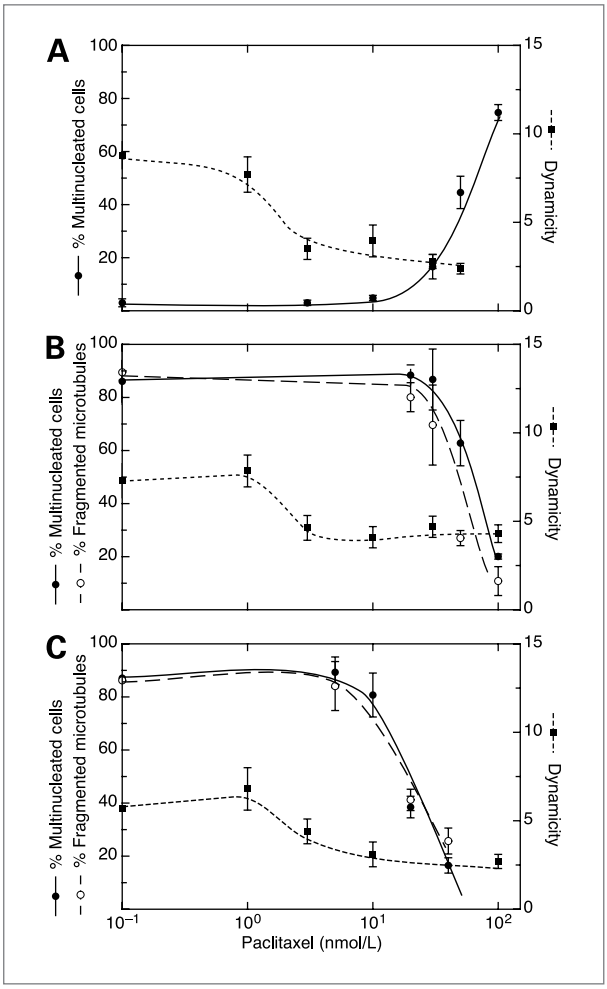

Figure 3. Effect of paclitaxel on cell division, microtubule fragmentation, and microtubule dynamics. WT cells (A), Tax 18 (B), and Tax 11-6 (C) were incubated with increasing concentrations of paclitaxel for 2 d. Each culture was then tested for the percentage of cells that were multinucleated (a measure of cells that were unable to complete cell division; ●), the percentage of cells with fragmented microtubules (○), and dynamicity (a measure of dynamic behavior; ■). Values for a variety of parameters that describe the dynamic behavior can be found in Supplementary Tables S2 to S4.

Paclitaxel-dependent cell lines contain microtubule fragments

While searching for alternative mechanisms to explain the decreased microtubule content, we noted that the mutant cells contained microtubule pieces of varying length that were not attached to the centrosome (see arrowheads in Fig. 1). We refer to these nonattached microtubules as fragments. The fragments are unlikely to be artifacts of sample preparation because they were seen in similar numbers regardless of whether cells were pre-extracted or fixed directly in methanol, and because they seldom were seen in WT cells. Moreover, they disappeared when mutant cells were treated with paclitaxel at concentrations that restored normal cell division. To determine whether the generation of microtubule fragments might be playing a role in the mutant phenotype and its reversal by paclitaxel, we measured the percentage of cells with multinucleation and the percentage of cells with microtubule fragments as a function of drug

concentration. The graphs in Fig. 3 compare these numbers with dynamicity, one of the parameters that are commonly used to quantify microtubule dynamics (Supplementary Tables S2–S4). The maximum decrease in dynamicity for all three cell lines was elicited by 3 to 10 nmol/L paclitaxel, a concentration well below what was needed to produce multinucleation in WT cells or restore normal cell division in mutant cells. Moreover, for the mutant cell lines, the decrease in multinucleated cells exactly paralleled the decrease in cells with fragmented microtubules, indicating that the same paclitaxel concentration that prevented the generation of microtubule fragments also restored normal cell division (Fig. 3B and C). Similar results were obtained when we used cell proliferation or mitotic index instead of multinucleation to assess paclitaxel effects on cell division (data not shown). Thus, the ability of paclitaxel to restore the normal growth of mutant cells seems to be related to its ability to inhibit microtubule fragmentation rather than its ability to suppress microtubule dynamics.

Fragments are produced by microtubule detachment from centrosomes

Microtubule fragments were seen throughout the cytoplasm of mutant cells including areas near the cell periphery (see arrowheads in Fig. 1). Although the higher microtubule density in WT cells increased the difficulty of detecting similar fragments, very few were seen after careful focusing through the cytoplasm. Moreover, we did not see fragments in the less dense peripheral area of the cells or in the small fraction (<5%) of normally occurring large multinucleated cells that had less densely packed microtubules. We initially thought that incorporation of mutant tubulin might be weakening the microtubule lattice, leading to a propensity of the microtubule wall to break when under mechanical stress from bending or other strains. Because the binding of paclitaxel is thought to strengthen lateral interactions between protofilaments (19), we reasoned that this action of the drug might allow the microtubules to resist mechanical stress. To determine whether microtubules were indeed incurring breaks along their length, we carried out live cell imaging of microtubules labeled with EGFP-MAP4. Contrary to our expectations, there were very few instances where we could see microtubules break into smaller pieces (0.03/cell/min). Even when microtubules were bent into U-shaped structures, breaks were not seen. Moreover, the frequency of microtubule breaks was similar for all three cell lines and did not change with drug treatment.

In contrast to the low incidence of mechanical breaks in all three cell lines, microtubules were frequently seen to detach from the centrosome in mutant, but not WT, cells. Examples of microtubule detachment in the two mutant cell lines are shown in Fig. 4A. Detachment was stochastic. Cells could go for some time without a visible detachment and then have several occurrences in quick succession. Detachment also did not require microtubules of any special length. Sometimes, it occurred with long microtubules (Fig. 4A, top, arrows), whereas at other times, short newly nucleated microtubules were affected (Fig. 4A, bottom, arrows). Following detachment, microtubules remained stable for varying periods of time: Some immediately began to depolymerize, whereas others waited. Depolymerization

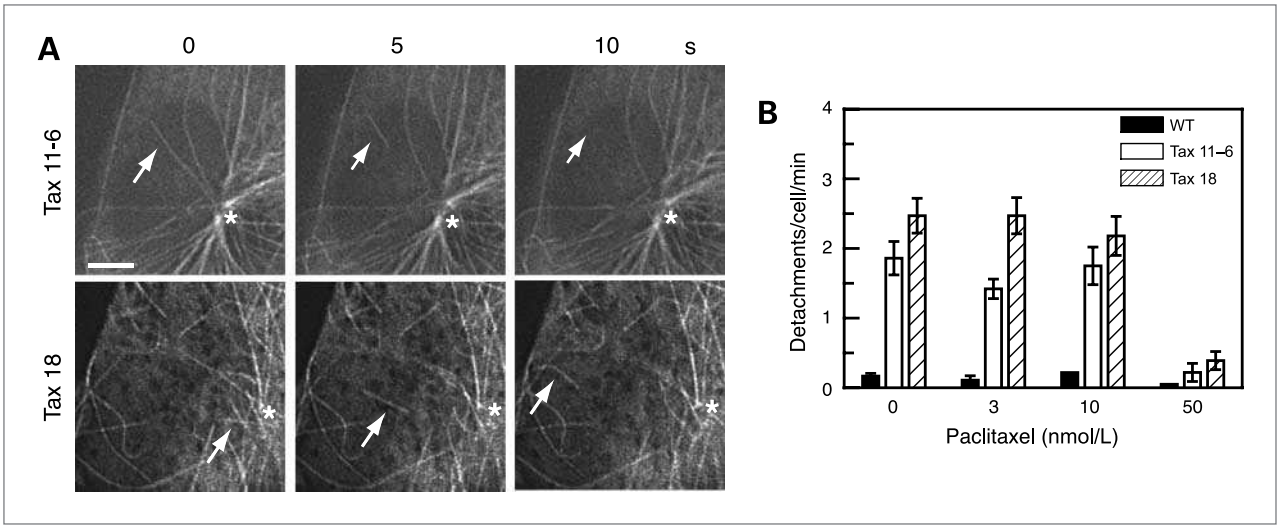

Figure 4. Microtubule detachment from centrosomes. A, paclitaxel-dependent mutants Tax 11-6 and Tax 18 were grown for 2 d without paclitaxel, transfected with *EGFP-MAP4*, and viewed by live cell imaging. Fluorescent images taken 5 s apart were deconvolved to improve contrast. Note detachment and shortening from the minus end of a long microtubule in Tax 11-6 (top, arrows), and detachment and translocation of a newly nucleated microtubule in Tax 18 (bottom, arrows). Asterisks mark the centrosomal area of the cells. Scale bar, 5 μm. B, cells treated with the indicated concentrations of paclitaxel for 2 d were viewed by time-lapse fluorescence microscopy. Microtubules that detached from the centrosome were counted from 25 to 40 min of time-lapse video recordings, representing five cells in two separate experiments, and the rate was calculated as the number of detachments/cell/min. Columns, mean; bars, SD.

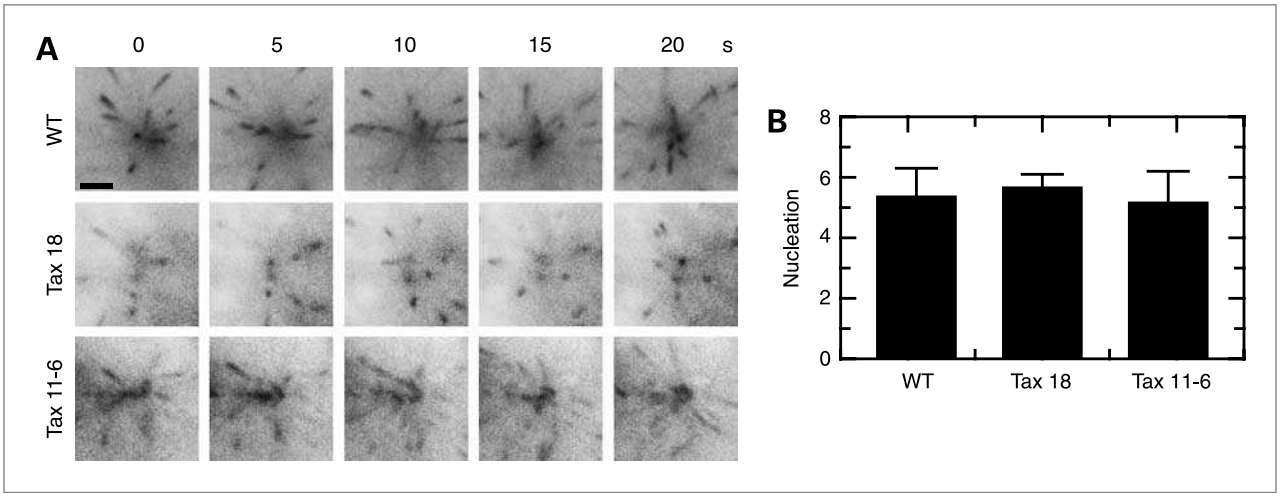

Figure 5. Microtubule nucleation. A, WT and mutant cells (Tax 18 and Tax 11-6) were grown for 2 d in the absence of paclitaxel, transfected with *EB1-GFP*, and viewed at 5-s intervals. Comets representing the plus ends of newly nucleated microtubules in the area around the centrosome are shown. Scale bar, 2 μm. B, comets newly appearing within a 30-μm^2 circular area around the centrosome were counted and averaged from 25 successive images in each of three to five separate cells. The *Y* axis represents the average number of comets per frame. Columns, mean; bars, SD.

occurred from either or both microtubule ends, causing them to have relatively short lifetimes and thereby appear as fragments of varying size in fixed cells. Although some of the fragments remained stationary during the period of observation, most translocated toward the cell periphery, thus accounting for the random distribution of fragments throughout the cytoplasm (Fig. 4A, bottom, arrows). The movement occurred at a velocity of ~10 μm/min, but we are unable at present to determine whether it is driven by molecular motors or by microtubule treadmilling.

Microtubule detachment also occurred in WT cells, but at a much lower frequency (Fig. 4B). The microtubule fragments that were produced exhibited similar behavior to what we observed in the mutant cell lines. Treatment with low paclitaxel concentrations that could inhibit microtubule dynamics had no effect on the frequency of microtubule detachment in any of the cell lines; however, treatment with 50 nmol/L paclitaxel, a concentration that inhibited WT cell division and largely rescued mutant cell division, strongly suppressed microtubule detachment in both WT and mutant cell lines (Fig. 4B). It thus seems that microtubule fragments are produced by microtubule detachment from centrosomes and that paclitaxel is able to inhibit this process.

Mutant cells nucleate microtubules at a normal rate

The high incidence of microtubule detachment in Tax 18 and Tax 11-6 raised the possibility that there could be a problem with the centrosome microtubule nucleating machinery. To address this possibility, we transfected all three cell lines to produce EB1-GFP (20), a protein that binds the plus ends of growing microtubules (21), and used live cell imaging to count the number of EB1-GFP trajectories in a circumscribed area around the centrosome. As shown in Fig. 5, we found no significant difference in the number of microtubules nucleated by WT and mutant cells. We conclude that the mutant cell lines are able to nucleate microtubules normally, but are unable to maintain stable microtubule attachments to the centrosome.

Discussion

Although microtubule-targeted drugs are powerful agents for treating cancer, patients often become refractory to therapy. In an effort to understand the mechanisms that allow cells to escape drug toxicity, we isolated hundreds of resistant cell lines that have mutations in α- or β-tubulin (6–8, 22–24). Based on the phenotypes of these resistant cells, we proposed a model in which mutant tubulins confer resistance by counteracting the action of the selecting drug on microtubule assembly. Thus, cells selected for resistance to colcemid, vinblastine, or other microtubule-destabilizing drugs have mutations in tubulin that stabilize microtubule assembly, whereas cells selected for resistance to paclitaxel or other stabilizing drugs have mutations in tubulin that destabilize microtubule assembly (25). Consistent with this model, cells selected for resistance to colcemid are cross-resistant to other destabilizing drugs, but are more sensitive to stabilizing drugs and have more of their tubulin assembled into microtubules. Conversely, cells selected for resistance to paclitaxel are cross-resistant to epothilones but are more sensitive to destabilizing drugs and have less tubulin assembled into microtubules. A subset of these latter mutants are cell lines that have very little assembled tubulin and whose proliferation is dependent on the presence of paclitaxel or other microtubule stabilizers (15). The exact mechanism by which these mutant cell lines arrive at their altered levels of polymerized tubulin, however, is not known.

An alternative to the idea that drugs inhibit cell division by altering microtubule stability and polymer levels posits that all mitotic inhibitors, regardless of whether they inhibit or promote microtubule assembly, act by suppressing microtubule dynamic instability (reviewed in ref. 3). According to this view, it is the ability of the drugs to inhibit the plus-end excursions of microtubules rather than their ability to alter net microtubule assembly that accounts for their capacity to block cell division. Although compatible with the well-known dynamic behavior of microtubules (2), this view fails to explain the observed cross-resistance/enhanced sensitivity patterns of tubulin mutants or the ability of microtubule stabilizers, but not destabilizers, to rescue paclitaxel-dependent mutants (25). An in-depth discussion of these alternative models for drug action can be found in a recent review (26).

In the studies described here, we attempted to resolve these differing views and elucidate the mechanism by which mutations cause paclitaxel dependence in two cell lines: one with a mutation in α-tubulin (Tax 11-6) and the other with a mutation in β-tubulin (Tax 18). We began by measuring a series of parameters that describe dynamic instability behavior, with the expectation that changes in one or more of these parameters would be able to explain the reduced microtubule assembly in these cells. We found that microtubule dynamics were partially suppressed in both mutant cell lines, but the changes in growth and shortening were insufficient to explain their greatly diminished microtubule assembly. Moreover, addition of paclitaxel at concentrations that increased microtubule assembly to more normal levels and allowed the cells to proliferate normally further suppressed microtubule dynamics rather than restoring behavior to normal.

In contrast to the small changes we measured in dynamic behavior, Tax 11-6 and Tax 18 had a 10- to 15-fold increase in the frequency of microtubule detachment from centrosomes compared with WT cells. Low concentrations of paclitaxel that suppressed dynamics did not affect the rate of microtubule detachment, but the higher drug concentrations that allowed normal cell division strongly inhibited detachment in the mutant cell lines and returned the rate to near-normal levels. The ability of paclitaxel to inhibit microtubule detachment from centrosomes is a drug action that has not previously been described. The increased microtubule detachment observed in the mutant cell lines produced unstable fragments that depolymerized rapidly and likely contributed to the reduced microtubule levels in those cells. Thus, even if altered microtubule polymer levels are not themselves the cause of paclitaxel dependence, they provide an accurate readout for changes in microtubule detachment that seem to be involved in the ability of the cells to proliferate.

Our results on the mechanism of drug dependence differ from a previous report that a paclitaxel-dependent A549 cell line exhibited increased microtubule dynamics that were suppressed to normal levels by paclitaxel treatment (27). The reasons for this discrepancy are not clear, but we point out that in contrast to our single-step mutants that are likely to differ from the WT by a single genetic lesion, the A549 mutant came from a multistep selection that could have introduced multiple mutations that contributed to the final phenotype. Moreover, if simply suppressing microtubule dynamics were sufficient to rescue the growth of those cells, they should have been rescued by drugs such as vinblastine or colchicine that also are known to suppress dynamics (28, 29); yet, that was not the case. Finally, we note that an immunofluorescence photograph (Fig. 4C; ref. 27) shows the presence of microtubule fragments, suggesting that microtubule detachment may also have contributed to the phenotype of the A549 mutant cell line.

Microtubule detachment is a poorly understood phenomenon whose mechanism is unknown. The release of microtubules from centrosomes was previously described in PtK1 and L929 cells, indicating that the process is not restricted to CHO cells (30, 31). Moreover, noncentrosomal microtubules are known to exist in differentiated muscle (32), neurons (33), and polarized epithelial cells (34), indicating that the release of microtubules from their nucleating centers may be an important biological process that can potentially occur by more than a single mechanism. A potential biological role of the phenomenon has come from the PtK1 study, where it was proposed that microtubule release might be involved in microtubule turnover (31). In support of this idea, we recently found that the rate of microtubule detachment in CHO cells is much higher during mitosis,[1] the same time that microtubule turnover is known to increase dramatically (35). We speculate that the production of microtubule fragments

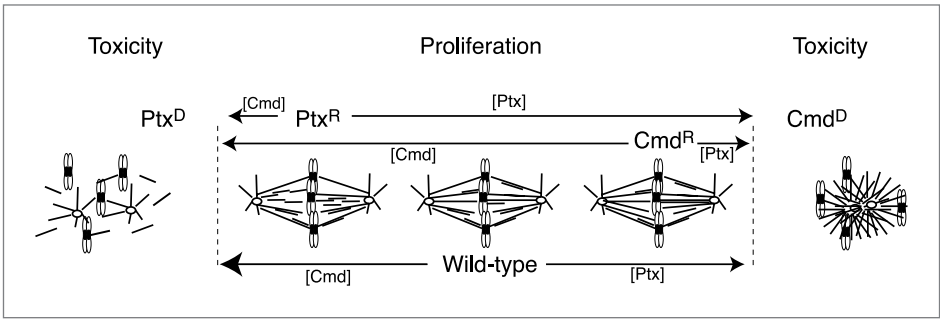

Figure 6. Model to explain drug resistance and dependence. Ptx^R, paclitaxel-resistant mutant; Ptx^D, paclitaxel-dependent mutant; Cmd^R, colcemid-resistant mutant; Cmd^D, colcemid-dependent mutant; [Cmd] or [Ptx], drug concentration. Dashed vertical lines, boundaries between normal proliferation and toxicity (defects in mitosis and cell division).

by detachment from spindle poles may be an important step in spindle assembly and function. This view is consistent with a previous study that used electron microscopy to trace microtubules through successive serial sections of PtK1 mitotic spindles and concluded that ~50% of the microtubules were unattached to spindle poles (36). More recent live cell imaging studies found evidence for microtubule release in mitotic LLPCK cells and showed that the fragments became incorporated into the central spindle (37, 38).

Taking these observations into account, we propose modifications to our previous model that used changes in microtubule polymer levels to explain drug resistance and dependence (25). The new model (Fig. 6) assumes that normal spindle function requires the incorporation of both continuous and fragmented microtubules in a proportion that falls within defined limits indicated by the dashed vertical lines in Fig. 6. Drugs exert toxicity when they reach concentrations (indicated by the size of the arrows in Fig. 6) that cause this proportion to fall outside of the normal limits. Thus, colcemid, vinblastine, and other microtubule-disrupting drugs become toxic by producing too many microtubule fragments, whereas paclitaxel, epothilones, and other microtubule-stabilizing drugs become toxic by inhibiting the formation of sufficient microtubule fragments. According to this model, tubulin mutations act by also changing the proportion of fragmented microtubules, but they do so in a direction that opposes the selecting drug. Thus, colcemid resistance mutations inhibit the production of microtubule fragments, thereby allowing the cells to tolerate more colcemid, vinblastine, and other drugs that promote the formation of fragmented microtubules in the mitotic spindle, but they tolerate less paclitaxel and other drugs that inhibit microtubule fragment formation. Paclitaxel resistance mutations would act in the opposite manner. In some cases, paclitaxel resistance mutations might cause so much microtubule fragmentation that mitotic spindle function is compromised and the cells are unable to divide. Tax 18 and Tax 11-6, which are paclitaxel dependent and become large multinucleated cells in the absence of drug, are examples of these more extreme mutations. The addition of paclitaxel, or other microtubule-stabilizing drugs, moves the proportion of fragmented microtubules back into the normal range and thus allows the cells to proliferate. Colcemid-dependent cells are also predicted by this model. Although such cells have not been directly isolated, cells that exhibit some dependency on colcemid for growth have been created by transfection and overexpression of DNA from a colcemid-resistant cell line (39).

The model is consistent with the properties of hundreds of drug-resistant cell lines we have examined, but much work remains to be done to establish its validity. Despite repeated attempts, we were not able to directly measure paclitaxel effects on microtubule detachment in mitotic cells because of their rounded morphology and the increased microtubule density and bundling caused by drug treatment. New methodologic approaches will have to be developed to address this question. Similarly, the mechanism of microtubule detachment is unknown. Our attempts to identify centrosomal proteins such as γ-tubulin and pericentrin at the minus ends of detached microtubules have thus far failed, suggesting that microtubule release might be caused by a regulated severing process rather than a "ripping out" process caused by instability of the anchoring complex. Proteins located at the centrosome that could potentially be involved in detachment include katanin and MCAK (40, 41). Finally, the role of microtubule fragments in mitotic spindle function is not clear. Although their existence has been known for many years, microtubule fragments have received little attention. Recently, however, a study in *Caenorhabditis elegans* suggested that fragments could be acting to increase microtubule density in the central spindle (42). Another report suggested that spindles can be viewed as tiled arrays of short microtubules linked together by motor proteins (43). Our studies add to these reports by showing that some tubulin mutations inhibit cell division by increasing the production of microtubule fragments. The demonstration that fragments are created by centrosomal release of microtubules and that the process is inhibited by drugs such as paclitaxel provides new impetus for further investigations into this emerging area.

Disclosure of Potential Conflicts of Interest

No potential conflicts of interest were disclosed.

Acknowledgments

We thank Dr. Xiangwei He for generously allowing us to use his microscope, Dr. Joanna Olmsted for providing us with *EGFP-MAP4*, and Dr. Lynne Cassimeris for making *EB1-GFP* available through Addgene.

Grant Support

NIH grant CA85935 (F. Cabral).

The costs of publication of this article were defrayed in part by the payment of page charges. This article must therefore be hereby marked *advertisement* in accordance with 18 U.S.C. Section 1734 solely to indicate this fact.

Received 06/10/2010; revised 09/01/2010; accepted 09/03/2010; published OnlineFirst 10/26/2010.

References

1. Wiese C, Zheng Y. Microtubule nucleation: γ-tubulin and beyond. J Cell Sci 2006;119:4143–53.
2. Kirschner M, Mitchison T. Beyond self-assembly: from microtubules to morphogenesis. Cell 1986;45:329–42.
3. Jordan MA, Wilson L. Microtubules as a target for anticancer drugs. Nat Rev 2004;4:253–65.
4. Cabral F. Mechanisms of resistance to drugs that interfere with microtubule assembly. In: Fojo AT, editor. Cancer drug discovery and

development: the role of microtubules in cell biology, neurobiology, and oncology. Totowa (NJ): Humana Press; 2008, p. 337–56.
5. Orr GA, Verdier-Pinard P, McDavid H, Horwitz SB. Mechanisms of Taxol resistance related to microtubules. Oncogene 2003;22: 7280–95.
6. Cabral F. Isolation of Chinese hamster ovary cell mutants requiring the continuous presence of taxol for cell division. J Cell Biol 1983;97: 22–9.
7. Schibler M, Cabral F. Taxol-dependent mutants of Chinese hamster ovary cells with alterations in α- and β-tubulin. J Cell Biol 1986;102: 1522–31.
8. Cabral F, Sobel ME, Gottesman MM. CHO mutants resistant to colchicine, colcemid or griseofulvin have an altered β-tubulin. Cell 1980; 20:29–36.
9. Laemmli UK. Cleavage of structural proteins during the assembly of the head of bacteriophage T4. Nature (Lond) 1970;227:680–5.
10. Minotti AM, Barlow SB, Cabral F. Resistance to antimitotic drugs in Chinese hamster ovary cells correlates with changes in the level of polymerized tubulin. J Biol Chem 1991;266:3987–94.
11. Jordan MA, Wilson L. Use of drugs to study role of microtubule assembly dynamics in living cells. Methods Enzymol 1998;298:252–76.
12. Gonzalez-Garay ML, Chang L, Blade K, Menick DR, Cabral F. A β-tubulin leucine cluster involved in microtubule assembly and paclitaxel resistance. J Biol Chem 1999;274:23875–82.
13. Cabral F, Barlow SB. Resistance to antimitotic agents as genetic probes of microtubule structure and function. Pharmacol Ther 1991; 52:159–71.
14. Kung AL, Sherwood SW, Schimke RT. Cell line-specific differences in the control of cell cycle progression in the absence of mitosis. Proc Natl Acad Sci U S A 1990;87:9553–7.
15. Barlow SB, Gonzalez-Garay ML, Cabral F. Paclitaxel-dependent mutants have severely reduced microtubule assembly and reduced tubulin synthesis. J Cell Sci 2002;115:3469–78.
16. Olson KR, McIntosh JR, Olmsted JB. Analysis of MAP 4 function in living cells using green fluorescent protein (GFP) chimeras. J Cell Biol 1995;130:639–50.
17. Jordan MA, Toso RJ, Thrower D, Wilson L. Mechanism of mitotic block and inhibition of cell proliferation by taxol at low concentrations. Proc Natl Acad Sci U S A 1993;90:9552–6.
18. Kamath K, Wilson L, Cabral F, Jordan MA. βIII-tubulin induces paclitaxel resistance in association with reduced effects on microtubule dynamic instability. J Biol Chem 2005;280:12902–7.
19. Downing KH. Structural basis for the interaction of tubulin with proteins and drugs that affect microtubule dynamics. Ann Rev Cell Dev Biol 2000;16:89–111.
20. Piehl M, Cassimeris L. Organization and dynamics of growing microtubule plus ends during early mitosis. Mol Biol Cell 2003;14:916–25.
21. Akhmanova A, Steinmetz MO. Tracking the ends: a dynamic protein network controls the fate of microtubule tips. Nat Rev Mol Cell Biol 2008;9:309–22.
22. Schibler MJ, Barlow SB, Cabral F. Elimination of permeability mutants from selections for drug resistance in mammalian cells. FASEB J 1989;3:163–8.
23. Hari M, Wang Y, Veeraraghavan S, Cabral F. Mutations in α- and β-tubulin that stabilize microtubules and confer resistance to colcemid and vinblastine. Mol Cancer Ther 2003;2:597–605.
24. Yin S, Bhattacharya R, Cabral F. Human mutations that confer paclitaxel resistance. Mol Cancer Ther 2010;9:327–35.
25. Cabral F. Factors determining cellular mechanisms of resistance to antimitotic drugs. Drug Resist Updat 2001;3:1–6.
26. Correia JJ, Lobert S. Molecular mechanisms of microtubule acting cancer drugs. In: Fojo AT, editor. Cancer drug discovery and development: the role of microtubules in cell biology, neurobiology, and oncology. Totowa (NJ): Humana Press, Inc.; 2008, p. 21–46.
27. Goncalves A, Braguer D, Kamath K, et al. Resistance to Taxol in lung cancer cells associated with increased microtubule dynamics. Proc Natl Acad Sci U S A 2001;98:11737–42.
28. Dhamodharan R, Jordan MA, Thrower D, Wilson L, Wadsworth P. Vinblastine suppresses dynamics of individual microtubules in living interphase cells. Mol Biol Cell 1995;6:1215–29.
29. Panda D, Daijo JE, Jordan MA, Wilson L. Kinetic stabilization of microtubule dynamics at steady state *in vitro* by substoichiometric concentrations of tubulin-colchicine complex. Biochemistry 1995; 34:9921–9.
30. Abal M, Piel M, Bouckson-Castaing V, Mogensen M, Sibarita JB, Bornens M. Microtubule release from the centrosome in migrating cells. J Cell Biol 2002;159:731–7.
31. Keating TJ, Peloquin JG, Rodionov VI, Momcilovic D, Borisy GG. Microtubule release from the centrosome. Proc Natl Acad Sci U S A 1997;94:5078–83.
32. Tassin AM, Maro B, Bornens M. Fate of microtubule-organizing centers during myogenesis *in vitro*. J Cell Biol 1985;100:35–46.
33. Ahmad FJ, Baas PW. Microtubules released from the neuronal centrosome are transported into the axon. J Cell Sci 1995;108:2761–9.
34. Bacallao R, Antony C, Dotti C, Karsenti E, Stelzer EH, Simons K. The subcellular organization of Madin-Darby canine kidney cells during the formation of a polarized epithelium. J Cell Biol 1989;109:2817–32.
35. Saxton WM, Stemple DL, Leslie RJ, Salmon ED, Zavortink M, McIntosh JR. Tubulin dynamics in cultured mammalian cells. J Cell Biol 1984;99:2175–86.
36. Mastronarde DN, McDonald KL, Ding R, McIntosh JR. Interpolar spindle microtubules in PTK cells. J Cell Biol 1993;123:1475–89.
37. Rusan NM, Fagerstrom CJ, Yvon AM, Wadsworth P. Cell cycle-dependent changes in microtubule dynamics in living cells expressing green fluorescent protein-α tubulin. Mol Biol Cell 2001;12: 971–80.
38. Tulu US, Rusan NM, Wadsworth P. Peripheral, non-centrosome-associated microtubules contribute to spindle formation in centrosome-containing cells. Curr Biol 2003;13:1894–9.
39. Whitfield C, Abraham I, Ascherman D, Gottesman MM. Transfer and amplification of a mutant β-tubulin gene results in colcemid dependence: use of the transformant to demonstrate regulation of β-tubulin subunit levels by protein degradation. Mol Cell Biol 1986; 6:1422–9.
40. Hartman JJ, Mahr J, McNally K, et al. Katanin, a microtubule-severing protein, is a novel AAA ATPase that targets to the centrosome using a WD40-containing subunit. Cell 1998;93:277–87.
41. Walczak CE, Mitchison TJ, Desai A. XKCM1: a Xenopus kinesin-related protein that regulates microtubule dynamics during mitotic spindle assembly. Cell 1996;84:37–47.
42. Srayko M, O'toole ET, Hyman AA, Muller-Reichert T. Katanin disrupts the microtubule lattice and increases polymer number in *C. elegans* meiosis. Curr Biol 2006;16:1944–9.
43. Yang G, Houghtaling BR, Gaetz J, Liu JZ, Danuser G, Kapoor TM. Architectural dynamics of the meiotic spindle revealed by single-fluorophore imaging. Nat Cell Biol 2007;9:1233–42.